Supplementary Information (SI) for CrystEngComm.
This journal is © The Royal Society of Chemistry 2024

Construction, structures, and magnetic studies of two cobalt(II) and nickel(II) coordination polymers displaying bex topology

Si-Tong Wu, [a] Zhijun Ruan, [a] Zhengfang Tian, *[a] Le Shi, [b] Jiong Yang, [c] and Dong Shao *[a]

[a] *Hubei Key Laboratory of Processing and Application of Catalytic Materials, College of Chemistry and Chemical Engineering, Huanggang Normal University, Huanggang 438000, P. R. China*

[b] *Key Laboratory of the Ministry of Education for Advanced Catalysis Materials, Zhejiang Key Laboratory for Reactive Chemistry on Solid Surfaces, Zhejiang Normal University, Jinhua, China*

[c] *Hubei Key Laboratory of Pollutant Analysis & Reuse Technology, College of Chemistry and Chemical Engineering, Hubei Normal University, Huangshi 435002, China*

Correspondence and requests for materials should be addressed to

Email: shaodong@nju.edu.cn

Table of Contents

EXPERIMENTAL SECTION

Physical measurements

Infrared spectra were obtained in the range of 600–4000 cm^{-1} on a Bruker tensor II spectrometer. Elemental analyses of C, O, and H were performed at an Elementar Vario MICRO analyzer. Variable-temperature powder X-ray diffraction data (PXRD) were recorded on a Bruker D8 Advance diffractometer with Cu Kα X-ray source (λ = 1.54056 Å) operated at 40 kV and 40 mA between 5 and 35° (2θ). Thermal gravimetric analysis (TGA) was carried out on freshly filtered crystals using the Mettler Toledo TGA2 instrument in an insert Ar atmosphere over a temperature range of 27–700 °C with a heating rate of 10 °C/min. N_2 and CO_2 isotherms were recorded using Quadrasorb automatic volumetric instrument in a clean ultra-high vacuum system with a diaphragm and turbo pumping system. Before measurement, the samples were loaded into the sample baskets within the adsorption instrument and then degassed under dynamic vacuum at 100 °C for 24 hours to obtain activated samples.

Magnetic Measurements.

Magnetic susceptibility measurements from 2 to 300 K with dc field up to 70 kOe were performed using a Quantum Design SQUID VSM magnetometer on the grounded powders from the single crystals of the compounds. Alternative current (ac) magnetic susceptibility data were collected in zero direct current (dc) field or 1000 Oe dc field in the temperature range of 2-8 K, under an ac field of 2 Oe, oscillating at frequencies in

the range of 1-1000 Hz. All magnetic data were corrected for the diamagnetism of the sample holder and of the diamagnetic contribution of the sample using Passcal's constants.

X-ray Crystallography

Single crystal X-ray diffraction data were collected on a Bruker D8 QUEST diffractometer with a PHOTON III CMOS detector (Mo-K_α radiation, $\lambda = 0.71073$ Å). The APEX III program was used to determine the unit cell parameters and for data collection. The data were integrated and corrected for Lorentz and polarization effects using SAINT.[S1] Absorption corrections were applied with SADABS.[S2] The structures were solved by direct methods and refined by full-matrix least-squares method on *F*2 using the SHELXTL[S3] crystallographic software package integrated in Olex 2.[S4] All the non-hydrogen atoms were refined anisotropically. Hydrogen atoms of the organic ligands were refined as riding on the corresponding non-hydrogen atoms. Additional details of the data collections and structural refinement parameters are provided in Table 1. Selected bond lengths and angles of **1** and **2** are listed in Table S1, S2. CCDC numbers 2376992 and 2376993 are the supplementary crystallographic data for this paper. They can be obtained freely from the Cambridge Crystallographic Data Centre via www.ccdc.cam.ac.uk/data_request/cif.

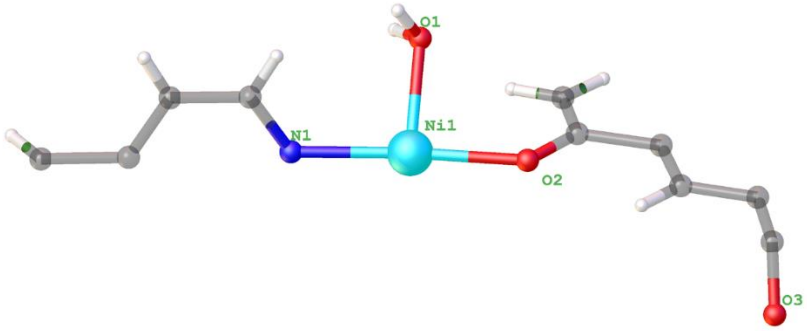

Figure S1. Asymmetry unit of **1**.

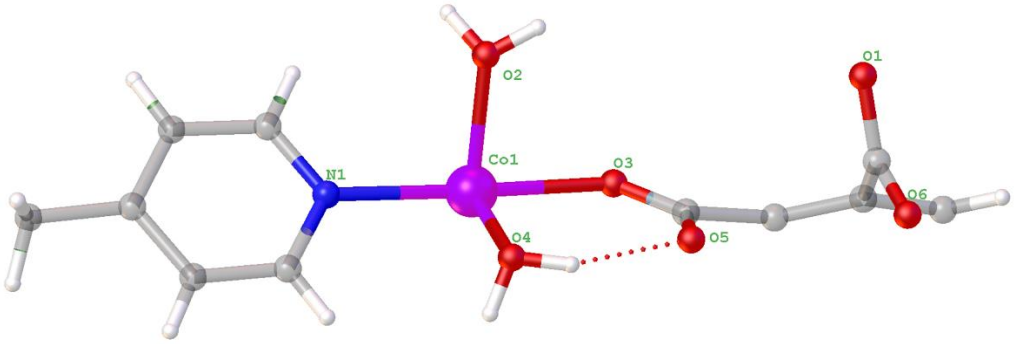

Figure S2. Asymmetry unit of **2**.

Table S1. Selected bond lengths (Å) in the **1** and **2**.

1		**2**	
Ni1-O1	2.0482(17)	Co1-O1*	2.2555(15)
Ni1-O1*	2.0482(17)	Co1-O4	2.0536(15)
Ni1-O2	2.048(2)	Co1-O6*	2.1586(15)
Ni1-O3$^{\#}$	2.1312(16)	Co1-O3	2.1586(15)
Ni1-O3$^{\&}$	2.1312(16)	Co1-O2	2.0294(16)
Ni1-N1	2.063(3)	Co1-N1	2.1226(17)
Ni-O/N	2.078	Co-O/N	2.129
Symmetry operation: *+X,1-Y,+Z; $^{\#}$1-X,+Y,1-Z; $^{\&}$1-X,1-Y,1-Z			

Table S2. Selected bond angles (Å) in the **1** and **2**.

1		**2**	
O1-Ni1-O1*	88.33(11)	O2-Co1-O3	86.49(7)
O1-Ni1-O3$^{\#}$	105.01(7)	O2-Co1-O4	99.68(7)
O1*-Ni1-O3$^{\#}$	165.84(7)	O2-Co1-N1	93.10(7)
O1*-Ni1-N1	93.96(8)	O2-Co1-O6*	154.94(6)
O2-Ni1-O1	90.28(7)	O2-Co1-O1*	98.57(6)
O2-Ni1-O3$^{\&}$	85.01(8)	O3-Co1-N1	176.02(6)
O2-Co1-N1	174.08(10)	O4-Co1-O3	90.10(6)
N1-Co1-O3$^{\&}$	89.90(8)	O4-Co1-N1	93.86(6)
N1-Co1-O3$^{\#}$	89.90(8)	O6*-Co1-O1*	59.09(5)

Table S3. Continuous Shape Measure (CShM) analysis for the **1** and **2**.

Compound, Metal center	CSM parameters* six-coordinated coordination sphere					Determined coordination geometry
	HP-6	PPY-6	OC-6	TPR-6	JPPY-6	
Ni	28.362	25.711	**1.802**	16.282	29.426	OC-6
Co	28.498	21.580	**2.294**	12.360	25.265	OC-6

*CShM [S5] parameters for six-coordinated complexes:

HP-6 - the parameter related to the hexagon (D_{6h});

PPY-6 - the parameter related to the pentagonal pyramid (C_{5v});

OC-6 - the parameter related to the octahedron (O_h);

TPR-6 - the parameter related to the trigonal prism (D_{3h});

JPPY-6 - the parameter related to the Johnson pentagonal pyramid (*C5v*).

Table S4. The possible hydrogen bonds in **1** calculated by PLATON.

D-H...A	d(D- H)	d(H...A)	d(D...A)	＜(DHA)
O(1)-H(1A)...O(3)	0.85	1.84	2.6859	171

Table S5. The possible hydrogen bonds in **2** calculated by PLATON.

D-H...A	d(D- H)	d(H...A)	d(D...A)	＜(DHA)
O(1)-H(1A)...O(4)	0.85	1.85	2.6552	157
O(1)-H(1B)...O(8)	0.85	2.21	2.8220	128
O(5)-H(5A)...O(25)	0.85	1.85	2.6505	157
O(5)-H(5B)...O(9)	0.85	2.21	2.8214	129
O(7)-H(7A)...O(9)	0.85	1.84	2.6326	154
O(7)-H(7B)...O(6)	0.85	1.91	2.7481	168
O(10)-H(10A)...O(8)	0.85	1.84	2.7481	155
O(10)-H(10B)...O(24)	0.85	1.92	2.7516	166

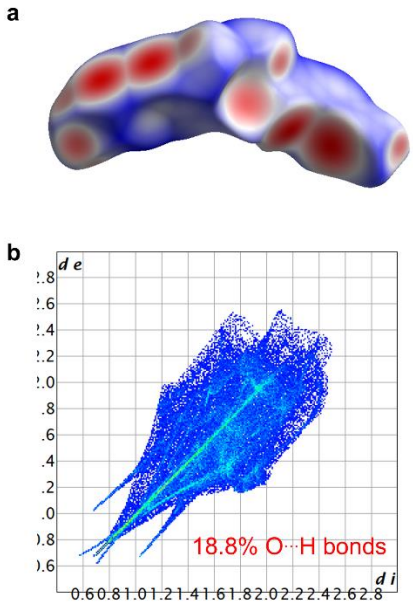

Figure S3. (a) View of the Hirshfeld surface mapped with d_{norm} properties for **1**; (b) Fingerprint plot for H-bond interactions in **1**.

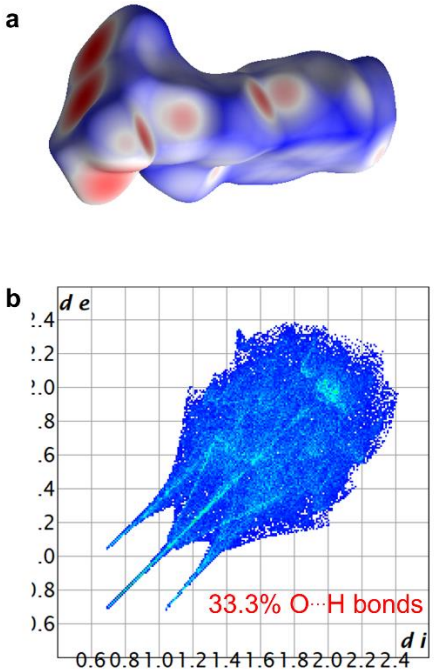

Figure S4. (a) View of the Hirshfeld surface mapped with d_{norm} properties for **2**; (b) Fingerprint plot for H-bond interactions in **2**.

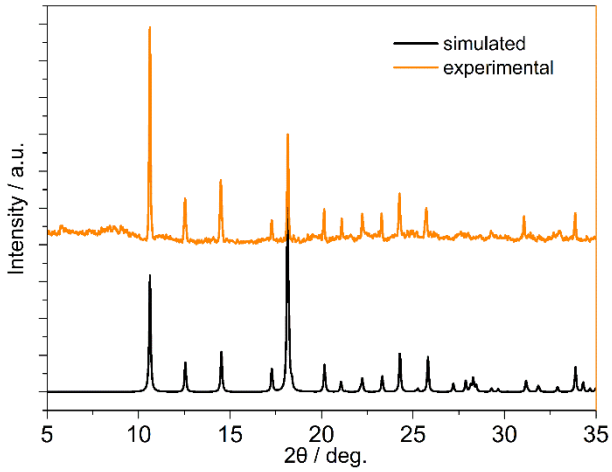

Figure S5. Comparison of the experimental PXRD pattern of **1** with the calculated pattern from single crystal data.

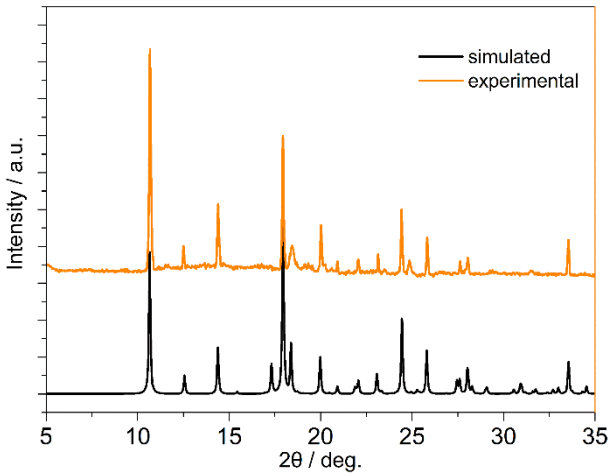

Figure S6. Comparison of the experimental PXRD pattern of **2** with the calculated pattern from single crystal data.

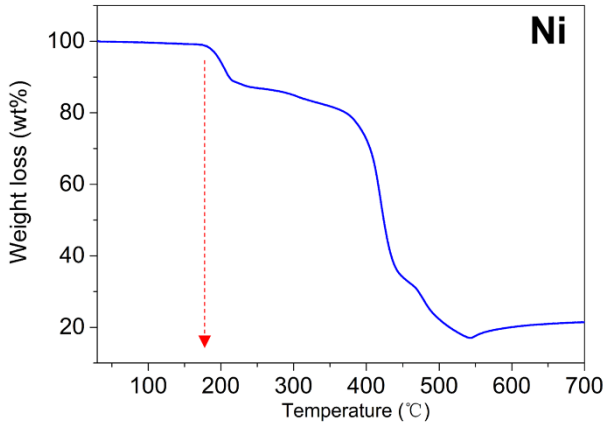

Figure S7. Thermogravimetric analysis curve of **1**.

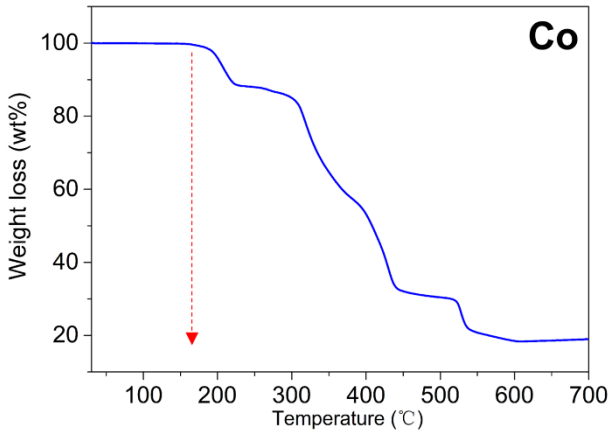

Figure S8. Thermogravimetric analysis curve of **2**.

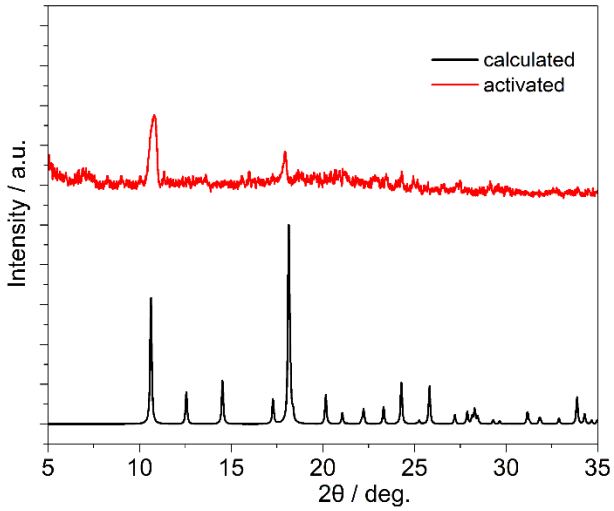

Figure S9. Comparison of the experimental PXRD pattern of activated sample of **1** with the calculated pattern from single crystal data.

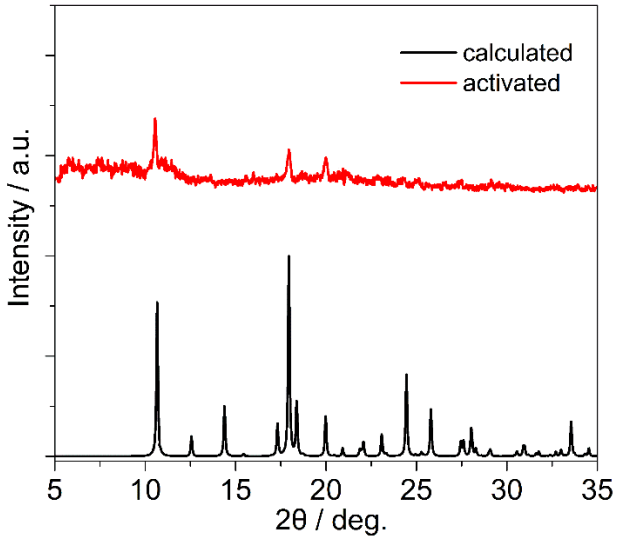

Figure S10. Comparison of the experimental PXRD pattern of activated sample of **2** with the calculated pattern from single crystal data.

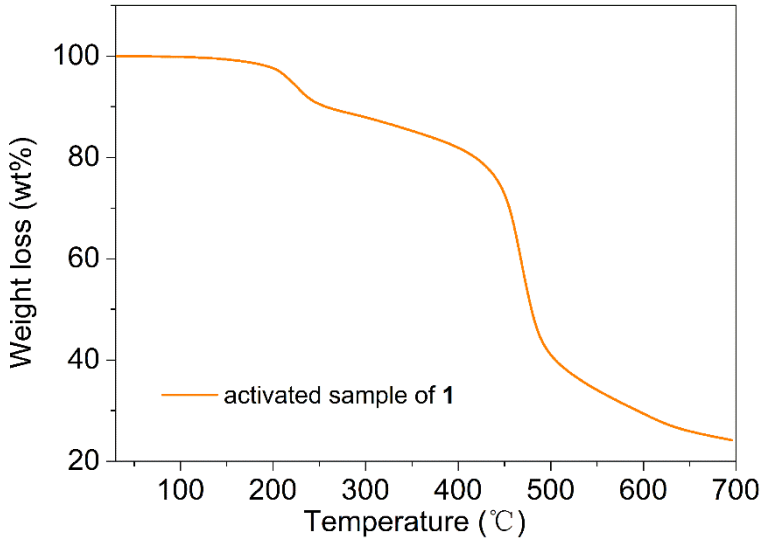

Figure S11. Thermogravimetric analysis curve of activated sample of **1**.

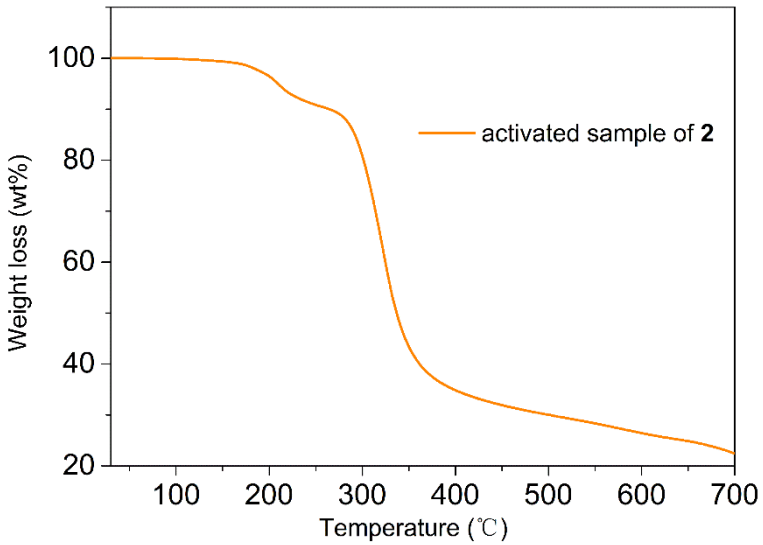

Figure S12. Thermogravimetric analysis curve of activated sample of **2**.

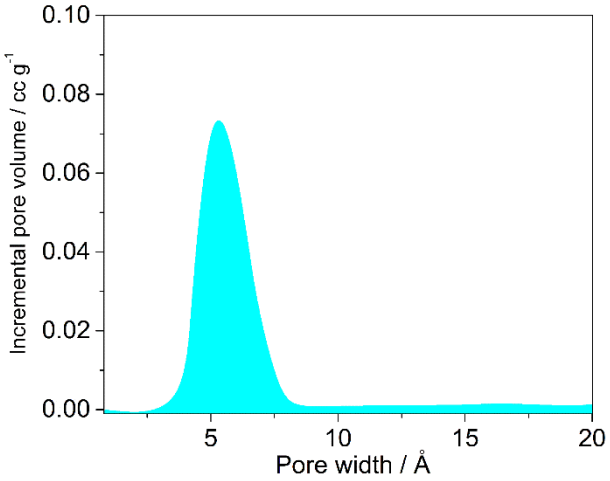

Figure S13. Pore size distribution (PSD) for **2** calculated from the CO_2 adsorption isotherm using Dubinin Asthakov (DA) methods.

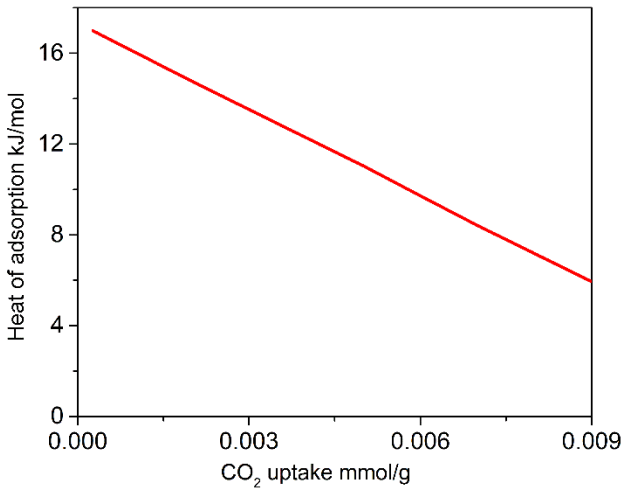

Figure S14. Heat of adsorption for **2**.

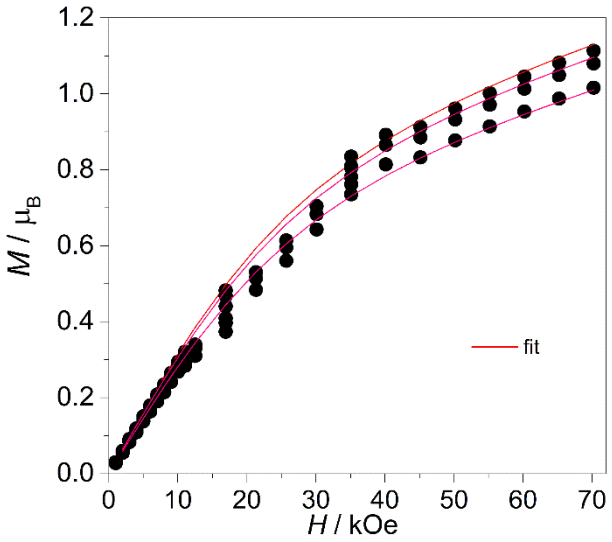

Figure S15. Field dependent magnetization for **1**.

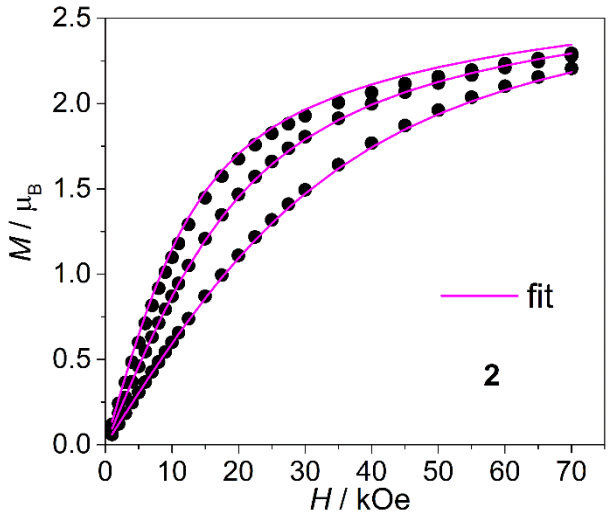

Figure S16. Field dependent magnetization for **2**.

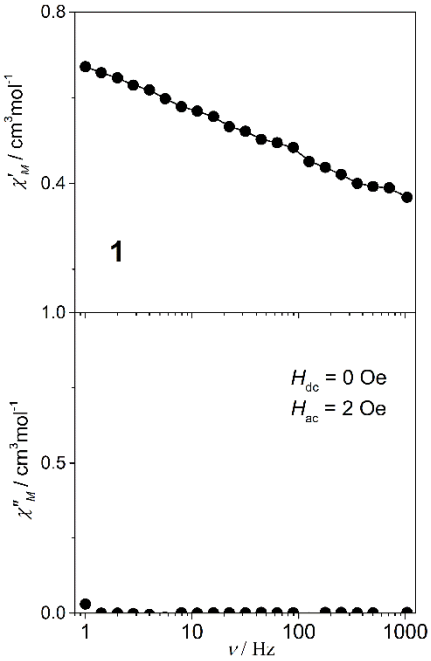

Figure S17. Frequency dependence of the ac susceptibilities measured under zero dc field at 1.8 K for **1**.

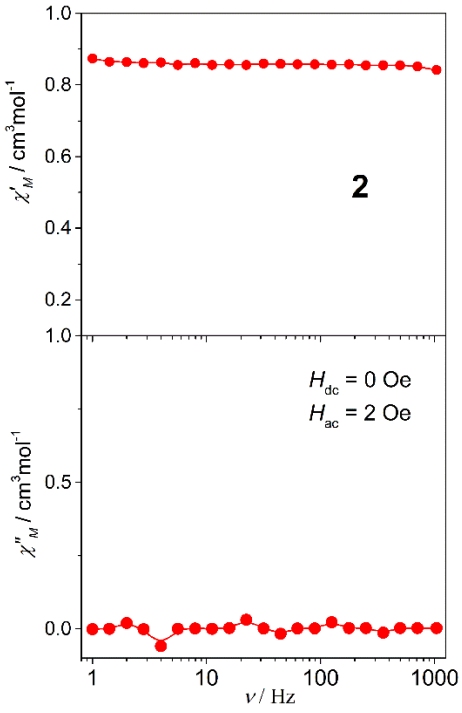

Figure S18. Frequency dependence of the ac susceptibilities measured under zero dc field at 1.8 K for **2**.

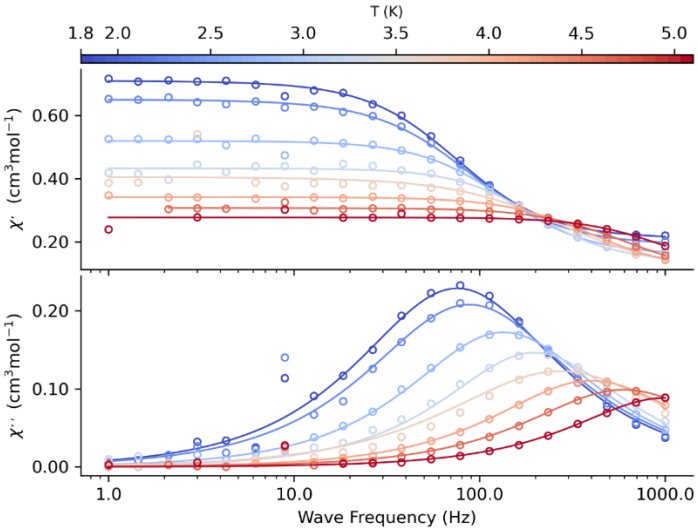

Figure S19. Frequency dependence of ac susceptibility measured under 1 kOe dc field for **2**.

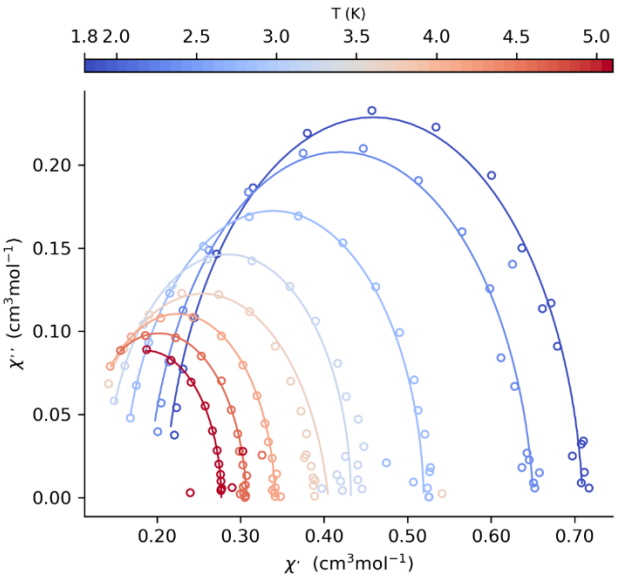

Figure S20. Cole-Cole plots of **2** obtained from 1 kOe dc field. The solid lines represent the best fits according to the generalized Debye model.

Table S6. Relaxation fitting parameters from the least-square fitting of the Cole-Cole plots of **2** under 1 kOe dc filed according to the generalized Debye model.

T / K	τ / s	χ_S / $cm^3mol^{-1}K$	χ_T / $cm^3mol^{-1}K$	α
1.79992	0.0021	0.20893	0.70973	0.05759
1.99979	0.00181	0.18789	0.65065	0.0681
2.49979	0.00119	0.15896	0.51949	0.02829
3.0001	8.08624E-4	0.13775	0.4322	0.00426
3.49846	5.86327E-4	0.10479	0.40507	0.12853
3.99897	4.00018E-4	0.10775	0.34148	0.03599
4.49696	2.66684E-4	0.09778	0.30706	0.03672
5.00051	1.59395E-4	0.09648	0.27712	0.01429

References

S1) SAINT Software Users Guide, version 7.0; Bruker Analytical X-Ray Systems: Madison, WI, 1999.

S2) G. M. Sheldrick, SADABS, version 2.03; Bruker Analytical X-Ray Systems, Madison, WI, 2000.

S3) G. M. Sheldrick, SHELXTL, Version 6.14, Bruker AXS, Inc.; Madison, WI 2000-2003.

S4) Dolomanov, O. V.; Bourhis, L. J.; Gildea, R. J.; Howard, J. A. K.; Puschmann, H. OLEX2: A Complete Structure Solution, Refinement and Analysis Program. *J. Appl. Crystallogr*., **2009**, 42, 339−341.

S5) M. Llunell, D. Casanova, J. Cirera, P. Alemany and S. Alvarez, SHAPE, version 2.1, Universitat de Barcelona, 2013.